JOURNAL OF APPLIED ELECTROCHEMISTRY **28** (1998) 491–501

# 304 Stainless steel oxidation in sulfate and sulfate + bicarbonate solutions

M. DROGOWSKA, L. BROSSARD*, H. MÉNARD

*Dépt. de Chimie, Université de Sherbrooke, Sherbrooke, Québec, Canada J1K 2R1 and * Institut de recherche d'Hydro-Québec (IREQ), Varennes, Québec, Canada J3X 1S1*

Received 20 August 1996; revised 10 June 1997

The electrochemical characterization of 304 stainless steel in 0.1–0.5 M $Na_2SO_4$ and $Na_2SO_4$ + $NaHCO_3$ aqueous solutions at pH ~8 was done in combination with SEM surface analysis. Passivation of the surface film without any pitting events is observed for the current–potential and current–time experiments, and no anodic current spikes, which are associated with depassivation events, are distinguishable above the background current level. However, SEM pictures of an electrode surface polarized at potentials above 0.4 V show microscopic pit nucleation. Even when the metal may be regarded as passive from a current–time or current–potential characteristics, passivity is not stable and localized film breakdown can still occur. The events are ascribed to pit nucleation at the active inclusion sites. The pits do not grow even into the metastable state but die through repassivation by metal salt precipitation immediately after birth. The effect is ascribed to the solubility of metal salts with the electrolyte produced by dissolution in the nucleation sites. The results show that pit nucleation and pit growth are two distinct processes. The importance of solution composition and the protective effect of bicarbonate ions is also discussed.

Keywords: *stainless steel oxidation*, *localized attack*, *stainless steel passivation*, *sulfate and bicarbonate ions*

## 1. Introduction

Despite extensive investigations, the processes involved in stainless steel corrosion remain poorly understood. Studies of the passivation and corrosion of stainless steel have generally been carried out in acidic or alkaline borate solutions. Borate has become a standard electrolyte for investigating passive film properties, although it is certainly not the type of solution found for most practical conditions. Pitting corrosion has generally been studied in chloride solutions. However, stainless steel passivation and corrosion in alkaline sulfate solutions have yet received little attention.

The anodic behaviour of iron in sulfate solutions [1–17] has been investigated and the passivation process was found to be highly inefficient [6]. Passivation appeared to be associated with a salt film precipitation and/or change in the solution pH close to the surface, which allows the formation of passive oxide [18–22]. The addition of a borate buffer to the neutral sulfate solutions increases passivation efficiency [6, 8, 16]. *In situ* enhanced Raman spectra obtained from the film formed on iron in the borate + sulfate solution indicate that the passive films are different from those formed in pure borate or pure sulfate solutions [15]. In mildly alkaline solutions, sulfate and borate anions are considered to be adsorbed onto the passive film surface, but not covalently bonded in the film as suggested for the film formed in a sulfate solution of pH 5 [15]. Still under discussion is the question of the passive film structure which can be amorphous or crystalline.

The corrosion of iron and low alloy steels exposed to the atmosphere is accelerated by the presence of sulfur dioxide, and sulfates and carbonate, after oxides and hydroxides, are the most frequently reported constituents of rust layers. It was acknowledged that the corrosion is usually localized; the sulfate anions are probably spatially heterogeneous and they accumulate to create 'sulfate nests' [2, 3, 7, 11]. In the initial stage, the surface is covered with a great number of small sulfate nests; the nests grow larger with exposure times and their number per unit area decreases. The sulfate nests contain high concentration levels of corrosion products and electrolyte while the pH value and the redox potential become low, which are the conditions that favour the local attack of the steel surface. The pH drops in local sites owing to the hydrolysis of the dissolved cations and the surrounding area acts as a cathode because of good electronic conductivity of the surface film.

Electrochemical behaviour of 304 stainless steel (SS304) in $Na_2SO_4$ and $Na_2SO_4$ + $NaHCO_3$ aqueous solutions at pH ~8 is investigated in the present study. Special attention is paid to the role of sulfate ions in passivation and corrosion processes. It is shown that the addition of bicarbonate to alkaline $Na_2SO_4$ solutions has an influence on the anodic behaviour of SS304, with the extent of this influence increasing

with the $NaHCO_3$ concentration. The potentiostatic method and weak galvanostatic polarization for determining the stability of the SS304 electrode surface were combined with SEM surface analysis. The results are discussed with a focus on relating pitting theories with electrochemical behaviour of the SS304 surface. The effect of the bicarbonate on SS304 electrochemical behaviour in the transpassive region before oxygen evolution is also considered.

## 2. Experimental details

The working electrode was made of austenitic 304 stainless steel (SS304) with the following chemical composition (wt %): C 0.009, Mn 1.67, P 0.034, S 0.020, Si 0.51, Cu 0.35, Ni 8.2, Cr 19.4, V 0.07, Mo 0.30, Co 0.14, Sn 0.018, Al 0.006, Ti 0.006, Nb 0.033 and the balance, Fe. The SS304 rod was machined in the shape of a cylinder and the experiments were carried out on the top of the cylinder in a meniscus position, with an exposed surface area of 0.19 $cm^2$. The electrode was mechanically polished with an alumina suspension to a mirror-like finish and rinsed with distilled water. This surface was examined before and after each experiment using a Bausch & Lomb optical microscope (70×). At the beginning of each experiment, the electrode was immersed in the solution and cathodically polarized at −0.8 V for 60 s for the purpose of removing as much surface oxides as possible. The auxiliary electrode was a platinum grid, while a saturated calomel electrode (SCE) connected to the cell by a bridge with a Luggin capillary served as the reference electrode; all potentials quoted in the paper refer to this electrode. The experiments were performed in a Faraday cage.

The solutions were prepared using analytical grade materials (BDH) and deionized water. The pH value was about 8, which was adjusted by adding NaOH. The cell capacity was about 600 ml, which ensured that the buildup of dissolved ions in the bulk of the solution during the course of a given experiment would be negligible. All solutions were deaerated using high-purity nitrogen before each experiment and a flow of nitrogen was established above the solution during the measurements. The experiments were performed at 25 and 50 °C.

## 3. Results and discussion

### 3.1. *Sulfate solutions*

Figure 1 shows potentiodynamic traces of an SS304 electrode in 0.1 and 0.5 M $Na_2SO_4$ solutions at 5 mV $s^{-1}$ (pH ~8). Prior to the potential sweep, the electrode was reduced at −0.8 V for 60 s but the passive film formed on the electrode was not completely reduced, regardless of the cathodic potential applied. The polarization curves display a large passive region of 1.2 V which extends to 0.4 V, at which point the anodic current begins to increase, reaches a maximum, and a second passive region appears before the oxygen evolution at 1.2 V. The anodic and cathodic currents slightly increase with the sulfate concentration from 0.1 to 0.5 M or at temperatures from 25 to 50 °C. Recently, *in situ* surface enhanced Raman spectra performed on 308 stainless steel in a borate solution in the low potentials passive region were associated with the formation of a highly protective mixture of oxy/hydroxide species of chromium, nickel and iron [23, 24]. The anodic current increases at about 0.4 V, the oxidation of Cr(III) to Cr(VI) forms a readily soluble oxide; $CrO_4^{2-}$ ions and some Cr(VI) species may be incorporated into the surface film without dissolution [25]. It is interesting to note that the integral Cr(III) oxy/hydroxy content may decrease from 70% at −0.2 V to only 25% at +0.6 V [26].

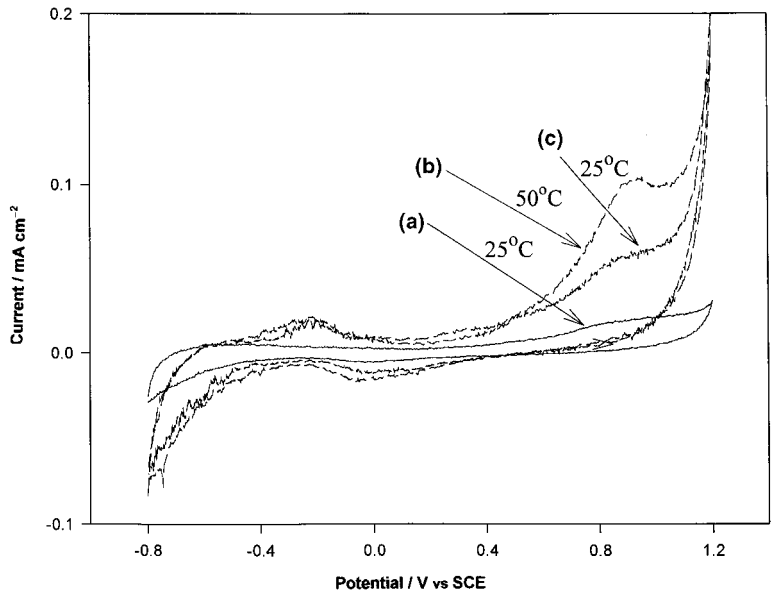


Fig. 1. Potentiodynamic curves for an SS304 electrode (0.19 $cm^2$) $dE/dt = 5\,mV\,s^{-1}$ in: (a) 0.1 M $Na_2SO_4$ solutions at 25 °C; (b) 0.1 M $Na_2SO_4$ solutions at 50 °C; and (c) 0.5 M $Na_2SO_4$ solutions at 25 °C.

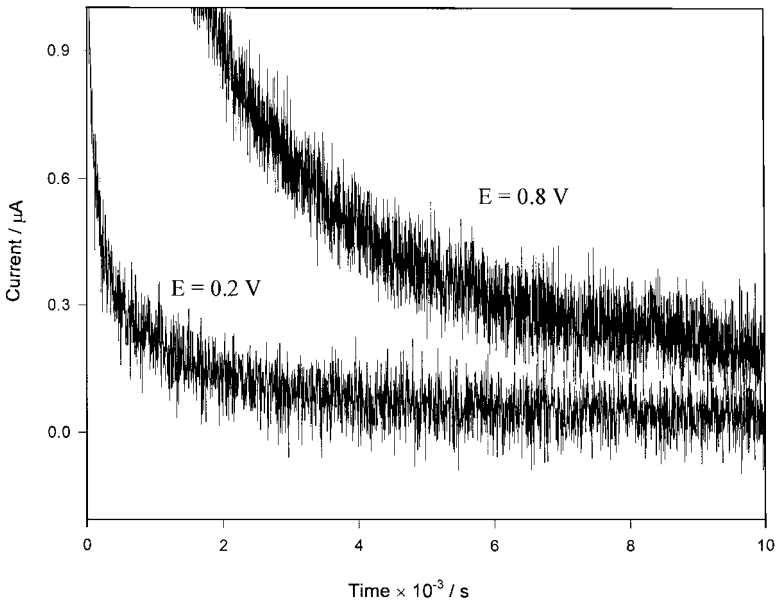


Fig. 2. Potentiostatic current–time transients performed on the SS304 electrode (0.19 $cm^2$) in a 0.1 M $Na_2SO_4$ solution at 0.2 and 0.8 V and at 25 °C.

Figures 2 and 3 show the current–time plots for the SS304 electrode in 0.1 M $Na_2SO_4$ solution at 0.2 and 0.8 V anodization potentials at 25 °C and 50 °C. For all cases, the oxidation current decays continuously with time as the electrode passivates, reaching a passive current of about 0.2 $\mu$A (~1.4 $\mu A\,cm^{-2}$) for a time close to 10 000 s. At no point did the anodic current show any sharp rise, and there was no indication that the anodic current might comprise a higher amplitude related to pit formation. The results present the weak anodic current mainly due to the homogeneous surface oxidation and passive film growth.

The current–time transients obtained by polarization of the SS304 electrode at 1 V for 0.1 and 0.5 M $Na_2SO_4$ solutions at 25 and 50 °C are illustrated in Figs 4 and 5. The shape of the current transient curves is similar to the one recorded at lower potentials (Figs 2 and 3), but the passive current of about 4 $\mu$A (~22 $\mu A\,cm^{-2}$) after 10 000 s is significantly higher at 1 V compared to the one at lower potentials. The experiments performed in both solutions (Figs 4 and 5) show the presence of anodic current spikes at 50 °C, not at 25 °C. Except for current spikes, the oxidation current is lower at 50 °C compared to 25 °C. The above results suggest acceptable passivity, consistent with the stability of $Fe_2O_3$ film. The similar shape of current–potential and current–time transients in 0.1–0.5 M $Na_2SO_4$ solutions, at 25 and 50 °C, for an applied potential ranging from 0.2 to 1 V indicates a similar passivation mechanism, irrespective of solution conductivity, temperature or oxidation potential.

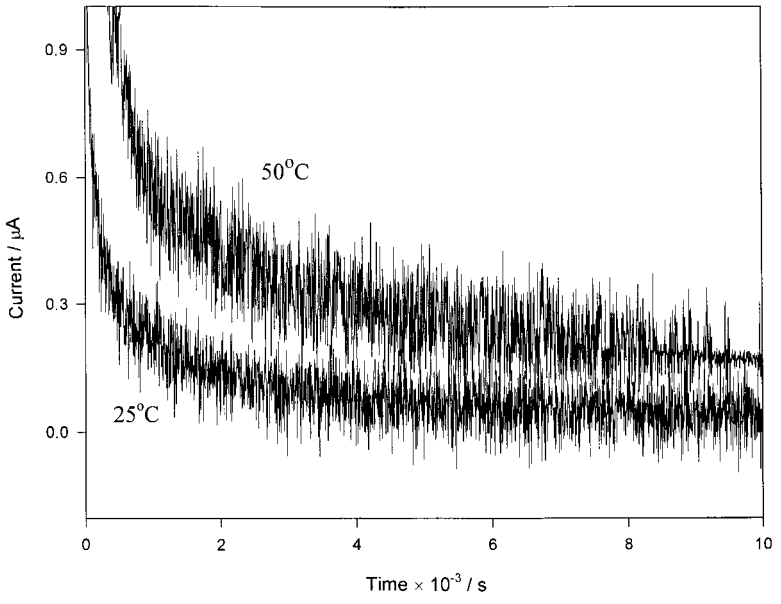


Fig. 3. As for Fig. 2 but at 0.2 V and at 25 and 50 °C.

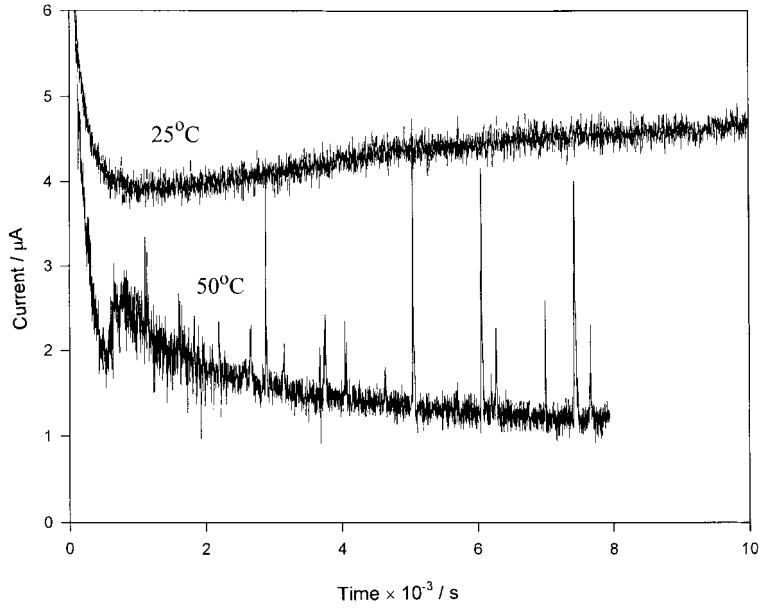


Fig. 4. Potentiostatic current–time transients performed on the SS304 electrode (0.19 cm$^2$) held at 1 V and at 25 and 50 °C in 0.1 M $Na_2SO_4$ solution.

SEM pictures of the SS304 surface in 0.1 and 0.5 M sulfate solutions at 25 and 50 °C, after polarization for 10 ks at 0.2, 0.6, 0.8 and 1 V are given in Figs 6–12. Some random precipitate on the surface is observed at 0.2 V in Fig. 6(a) (general surface picture) and Fig. 6(b) (precipitate finer resolution) although no localized attack with pitting was detected.

The electrode surface changed with the increase of potential and sulfate concentration. Although, the chromium oxy/hydroxy passive film is partially dissolved at 0.4 V, Figs 7b, 8d, 9b, 10c give examples of numerous deposits which were found on the mixed-oxides surface films, and a great number of microscopic pits (wholes) is observed on the SS304 surface (Figs 7(a), 8(a) and 11(a)). As shown in Fig. 7(a), in 0.5 M $Na_2SO_4$ at 0.6 V and 25 °C the pit occurrence is a random phenomenon which may be compared with the specially heterogeneous small 'sulfate nests' which do not grow further but die. A number of pit nuclei were found to be deposited on the surface in a flower-like form (Fig. 7(b)); the initiate pits formed micro-cavities that were evidently active for a brief period and then became repassivated (Fig. 7(c)). As the pits evolved toward a cylindrical shape, the ions produced by dissolution tend to diffuse away and precipitate in the centre, from the bottom to the top of the pit (Fig. 7(c)). The surrounding surface of the pit is almost free of precipitate (see Figs 7(b, c) and 8(b, c)). In 0.1 M $Na_2SO_4$ at 0.8 V and 25 °C, the pits are well developed (Fig. 8(a, b)); the pit initiation in Fig. 8(d) and evidently the precipitate species spread from the bottom to the top in Fig. 8(c). Under similar condi-

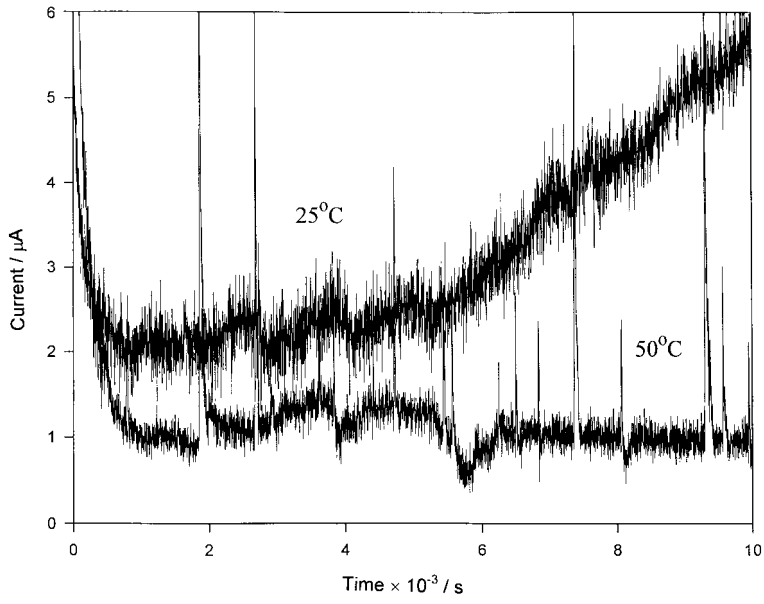


Fig. 5. As for Fig. 4 but in 0.5 M $Na_2SO_4$ solution.

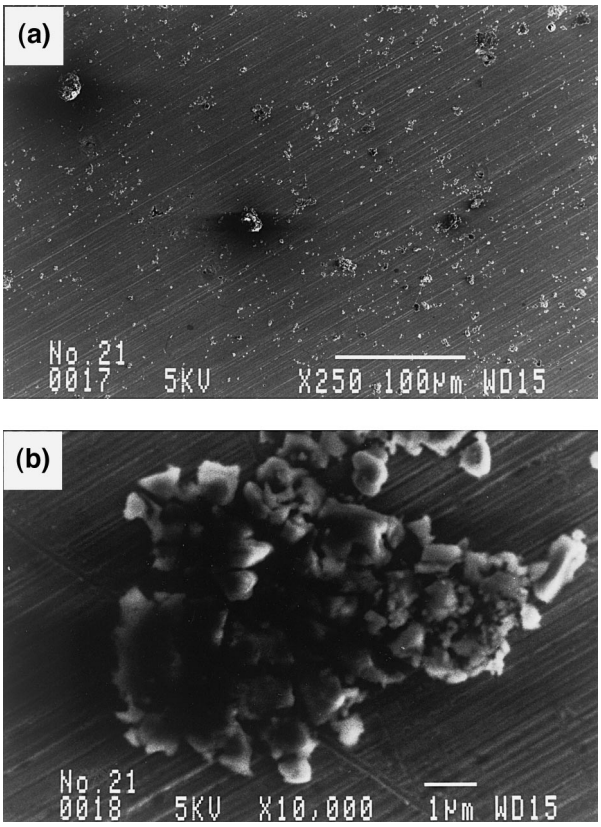


Fig. 6. SEMs for SS304 electrode surfaces after polarization at 0.2 V for 10 ks in 0.5 M $Na_2SO_4$ solution at 50 °C; (a) general surface image and (b) detailed precipitate finer resolution.

tions but at a temperature of 50 °C, the deposit increased and no evidence of pitting was noticed in Fig. 9(a, b). In 0.5 M $Na_2SO_4$ and at 25 °C the dense deposit (Fig. 10(b, c)) with the repassivated pit (Fig. 10(d)) is observed on the surface. The pit pictures on the electrode polarized at a potential of 1 V in 0.1 M and 0.5 M $Na_2SO_4$, at 25 and 50 °C are presented in Figs 11 and 12, respectively. Different kinds of pits are observed, with the dense precipitate on the surface surrounding the pit (Figs 11(b) and 12(a, b)). Pit repassivation begins from the surrounding deposit at the top edge of the pit (Figs 11(c) and 12(a, b)). The thick precipitate formed on the electrode protects the surface (Figs 11 and 12) and accounts for the quasipassive anodic current shown in Figs 4 and 5. Morphological observations show the different precipitation on the electrode surface in 0.5 M $Na_2SO_4$ and surface coloration of the passive film to a uniform gold colour could be seen with the naked eye. The coloration of passive film is associated with the optical phenomenon of multiple, thin layer beam interference [27, 28]. The surface coloration confirms the film thickening at a potential of 1 V.

The results presented above are consistent with the theory that pit nucleation and pit growth are two distinct processes [22, 29]. Pit nucleation is an unstable process and most events terminate at this stage. Pit nucleation may occur by chemical and electrochemical dissolution of inclusions under diffusion control. In particular, manganese sulfide inclusions play a major role as active surface sites [30–32]. The

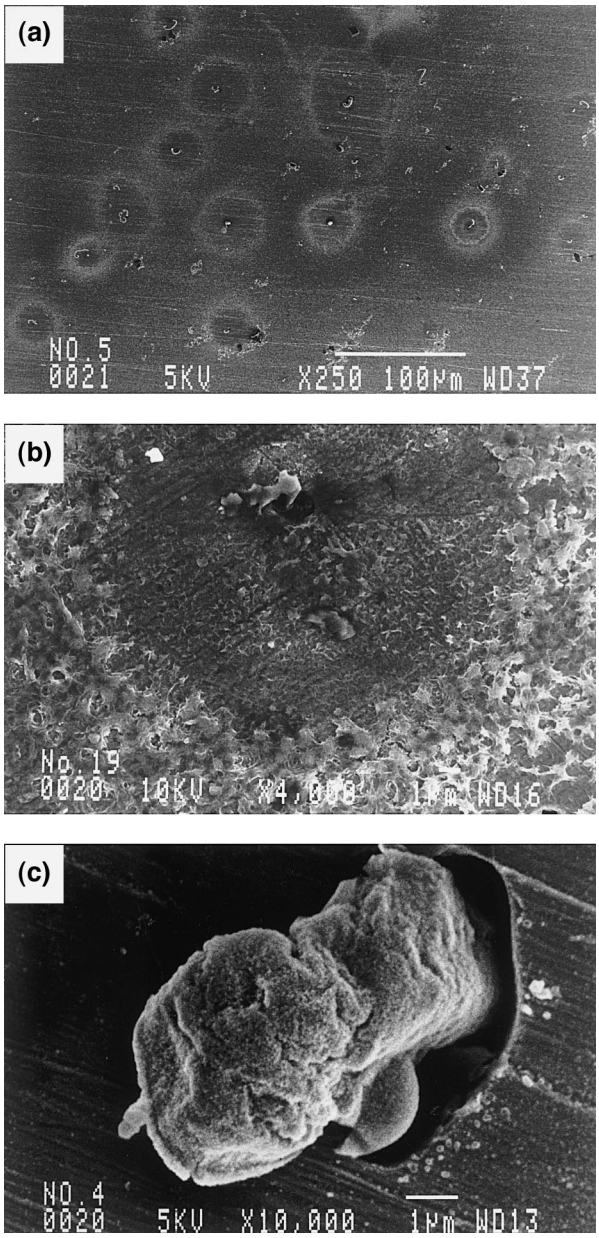


Fig. 7. SEMs for SS304 electrode surfaces after polarization at 0.6 V for 10 ks in 0.5 M $Na_2SO_4$ solution at 25 °C; (a) general surface image; (b) general pit picture; (c) pit with the precipitate inside, finer resolution.

present results indicate that in the presence of sulfate ions pits growth is inhibited by the formation of precipitate.

EDX analysis indicated an increase in manganese in the precipitate inside the holes. The increase in sulfur concentration was found on the surrounding surface of the top of the pit. No oxygen analysis could be done. The dissolution of large a number of small active inclusions (e.g. manganese [30–32]), could explain the pitting process on the electrode surface and could cause the oscillation of the anodic current. As illustrated in Figs 7(c) and 8(c), the metal salt precipitation starts at the bottom of a pit and spreads to the top. However, these pit nuclei, which do not exceed a few micrometre in diameter, do not spread on the surface but simply repassivate. The amount of dissolution products from these active

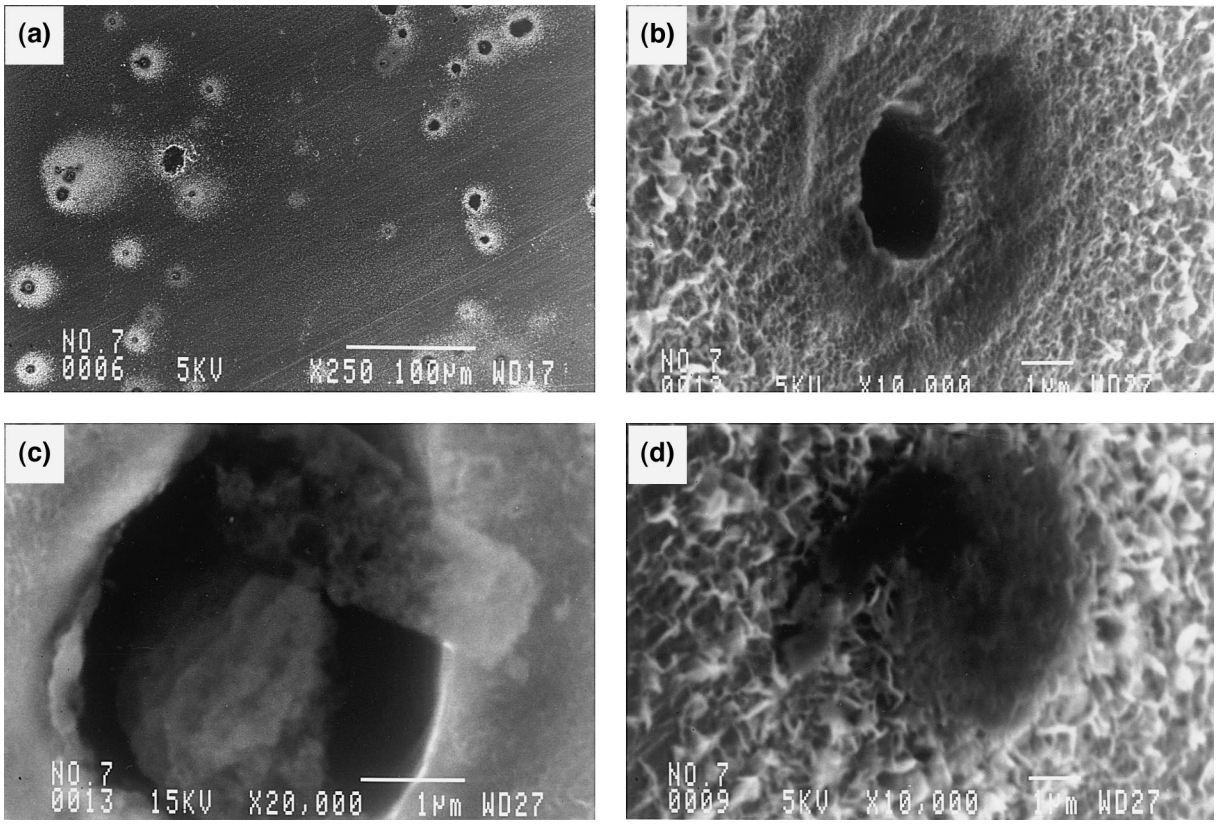


Fig. 8. SEMs for SS304 electrode surfaces after polarization at 0.8 V for 10 ks in 0.1 M $Na_2SO_4$ solution at 25 °C; (a) general surface image; (b) general pit picture; (c) pit with the precipitate inside, finer resolution; (d) pit initiation.

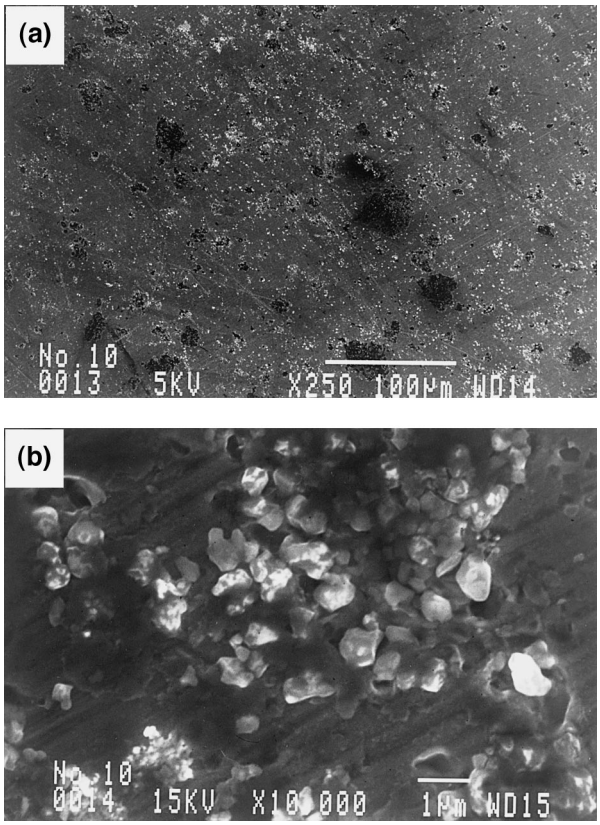


Fig. 9. SEMs for SS304 electrode surfaces after polarization at 0.8 V for 10 ks in 0.1 M $Na_2SO_4$ at 50 °C; (a) general surface image and (b) detailed precipitate finer resolution.

sites would necessarily be small and unstable followed by immediate precipitation and subsequent passivation by oxide film formation under the protective metal salt layer [18–22]. The salt precipitate film forms a barrier to the surface metal dissolution and allows a passive oxy/hydroxy film to be formed. The significant enhancement in the precipitation rate is observed at an oxidation potential of 1 V and with the increase of sulfate concentration (from 0.1 to 0.5 M) and the solution temperature (from 25 to 50 °C).

On the other hand, in sulfate solutions the process occurs at a low anodic current of about 0.8–4 $\mu$A, (4–21 $\mu A\,cm^{-2}$) without the current spikes typically observed when pitting is provoked by chloride ions [22, 33]. However, anodic currents of the order of some microamperes may result in a pit of some micrometres in size (e.g. 1 $\mu$A for 1 s corresponds to a pit of this dimension). It is postulated that in the presence of $SO_4^{2-}$ anions, the dissolution rate is so high that the salt film precipitates prior to the formation of the oxide film. The weak anodic current oscillations seem to represent a localized reactivation of the surface when metal dissolves through the oxide film followed by the passivation events under the salt film. Based on the magnitude of the current oscillations, it may be deduced that the pit nuclei were very small but the passivation was not complete since a weak residual current was always measured. For a pit to remain stable, the metal salt solution in the pit must

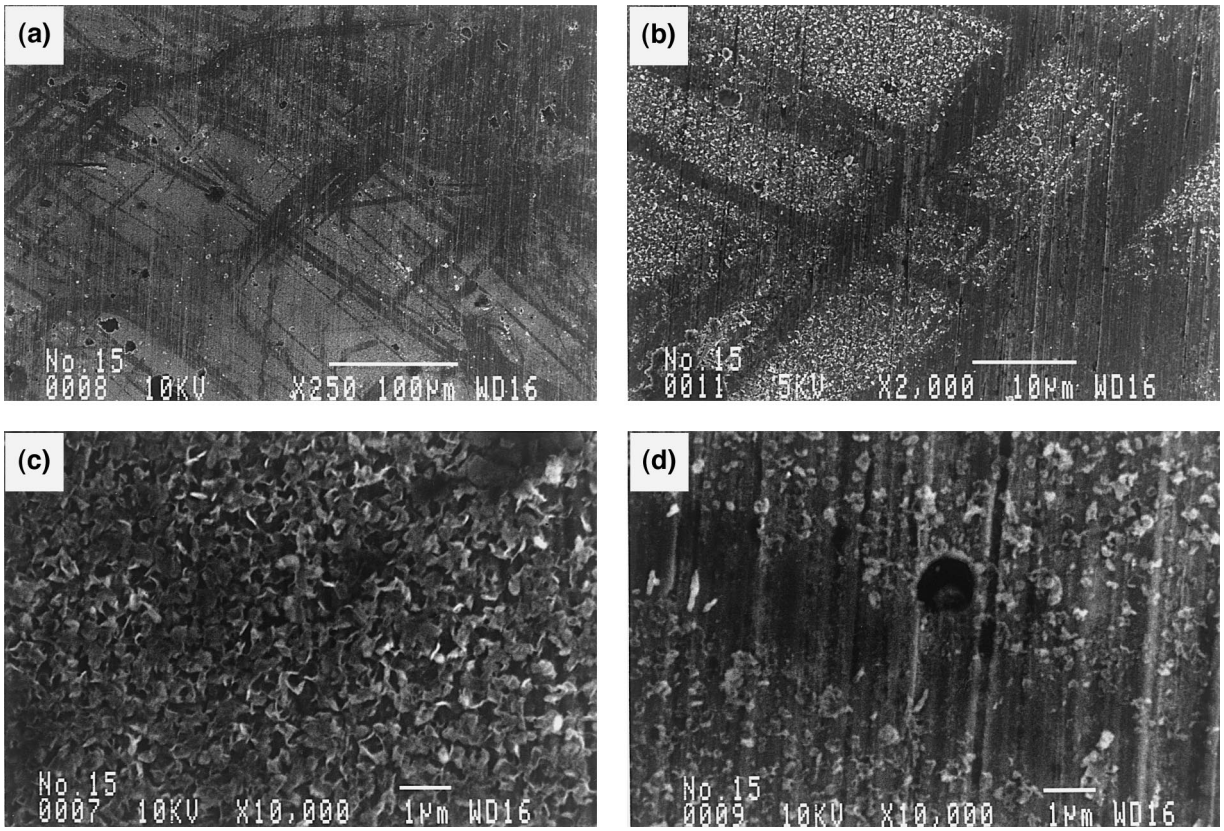


Fig. 10. SEMs for SS304 electrode surfaces after polarization at 0.8 V for 10 ks in 0.5 M $Na_2SO_4$ solution at 25 °C; (a) and (b) general surface image; (c) precipitate film finer resolution; (d) repassivated pit detail.

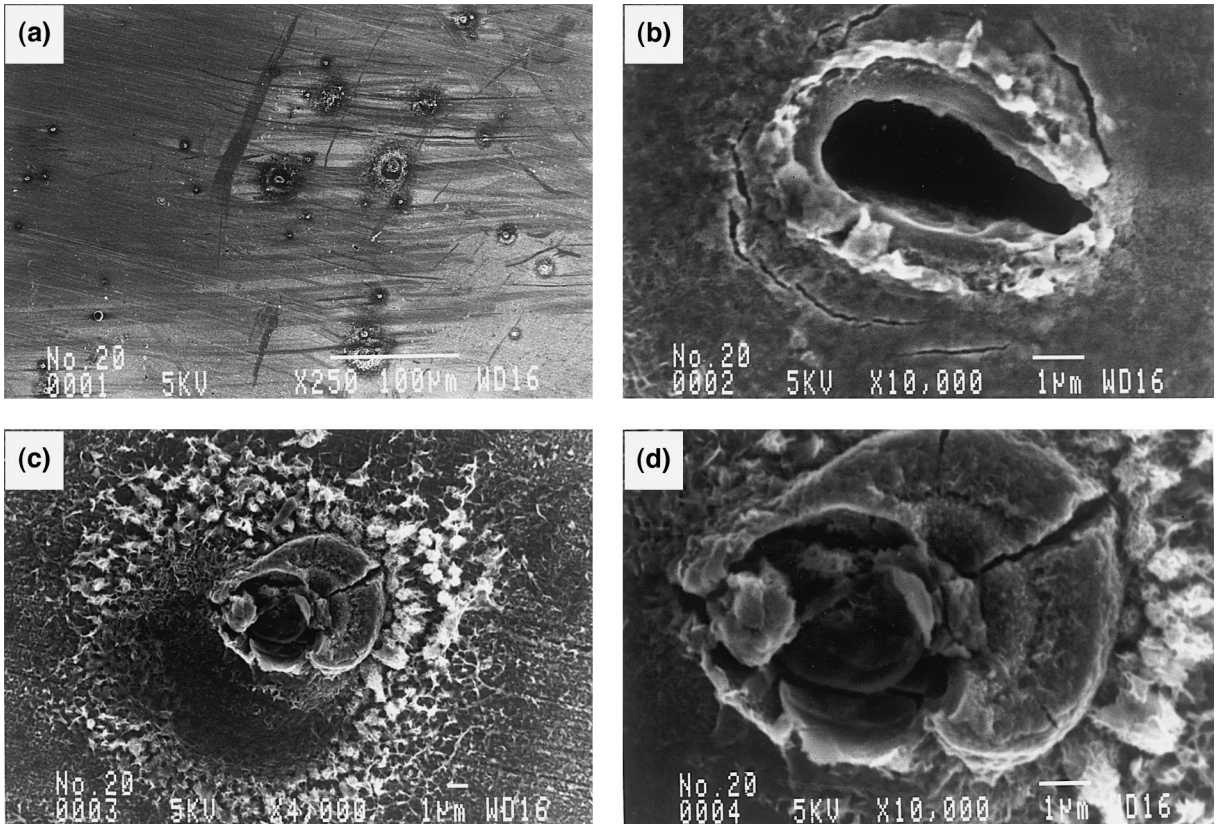


Fig. 11. SEMs for SS304 electrode surfaces after polarization at 1 V for 10 ks in 0.1 M $Na_2SO_4$ solution at 50 °C; (a) general surface image; (b) pit picture finer resolution; (c) and (d) flower-like form repassivated pit, finer resolution.

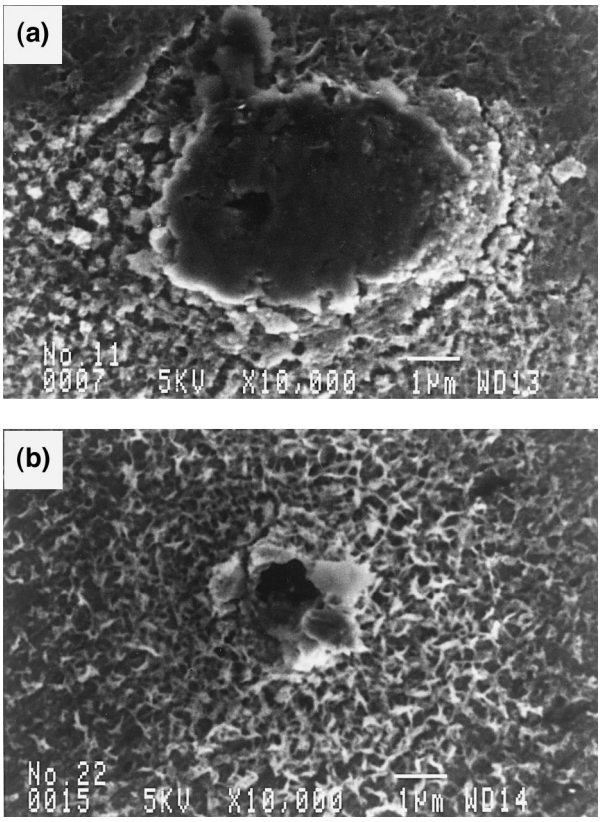


Fig. 12. SEMs for SS304 electrode surfaces after polarization at 1 V for 10 ks in 0.5 M $Na_2SO_4$ solution at 25 °C (two different sites).

be concentrated and some supersaturation is necessary prior to salt film precipitation. The reaction mechanism assumes that the sulfate migration through the existing oxide and precipitate passive films has to exist. Thus, metal salt is thought to be formed and the low passive current density itself implies that this solid nucleation would be a fast process.

The results show that, although the metal may be regarded as passive from a current–time or current–potential characteristics, passivity over the entire surface is not stable and localized breakdown still occurs: hence, pitting could start at any small defect in the oxide film. There is no *a priori* reason that the background noise level should be the lowest. The steel inclusions microstructure plays an important role in the pitting phenomenon, although the process involved in pit formation with an inner salt precipitation is specific to sulfate solutions.

### 3.2. *Effect of bicarbonate*

The electrochemical behaviour of the SS304 electrode in $Na_2SO_4$ + $NaHCO_3$ solutions at pH 8 and 25 °C is illustrated by the voltammograms in Fig. 13. Adding bicarbonate to $Na_2SO_4$ solutions had little effect at low potentials but resulted in substantial changes in transpassive potentials from about 0.9 V to the oxygen evolution.

The addition of 0.1 M bicarbonate to the 0.1 M sulfate solutions and at 0.8 V applied potential provokes a lower anodic current and requires less time to reach surface passivation, as illustrated by current–time transients at 25 °C in Fig. 14. The increase of temperature to 50 °C (Fig. 15) and sulfate concentration to 0.5 M (Fig. 16) gives the higher quasipassive anodic current. SEM images of the SS304 electrode surface after polarization for 10 ks at 0.8 V and 25 °C in 0.1 M $Na_2SO_4$ + 0.1 M $NaHCO_3$ (Fig. 17(a)) and 0.5 M $Na_2SO_4$ + 0.1 M $NaHCO_3$ (Fig. 17(b)) solutions are shown. In both solutions, thick film precipitate covers the electrode surface but in the case of higher sulfate concentration (Fig. 17(b)) the film is thicker and the pit well repassivated, but the deposit adjacent to the pit opening became slightly detached from the steel substrate (Fig. 17(b)).

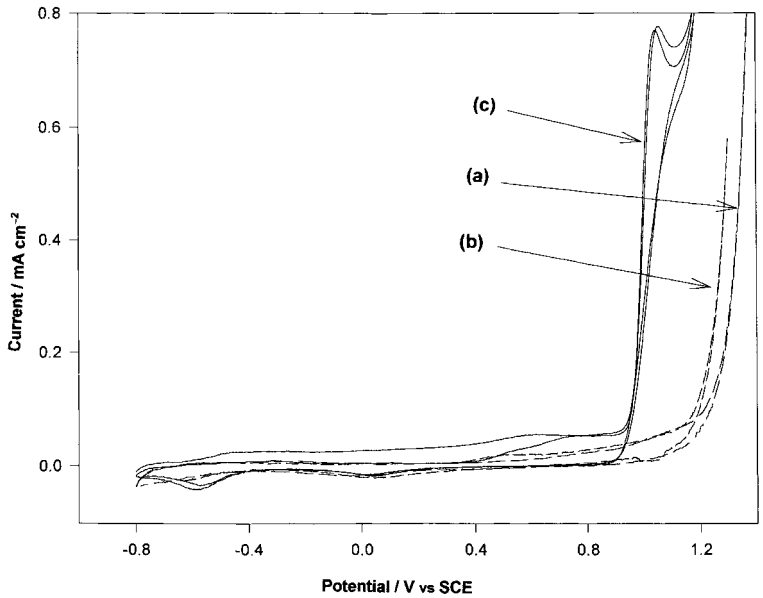


Fig. 13. Cyclic voltammograms for an SS304 electrode in (a) 0.1 and (b) 0.5 M $Na_2SO_4$ and (c) 0.1 M $Na_2SO_4$ + 0.1 M $NaHCO_3$ solutions, at $dE/dt = 5\,mV\,s^{-1}$ (pH 8, 25 °C).

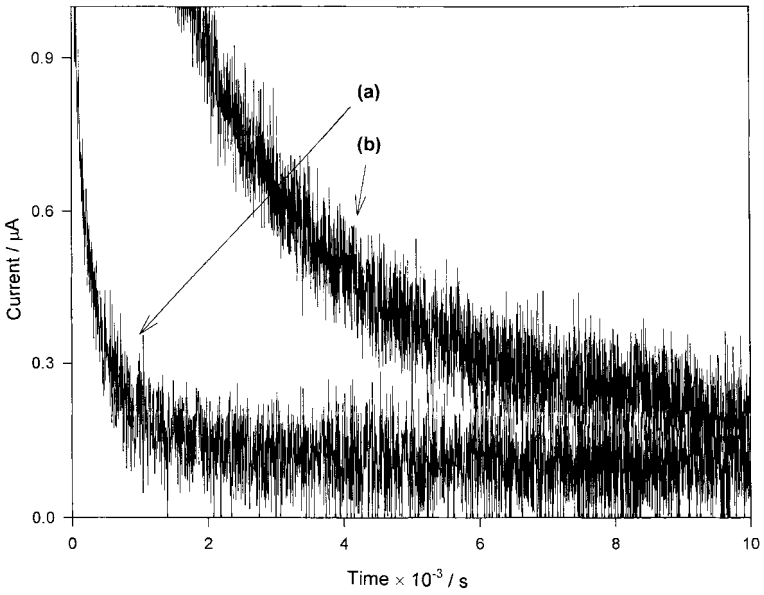


Fig. 14. Potentiostatic current–time transients for an SS304 electrode held at 0.8 V for 10 ks in (a) 0.1 M $Na_2SO_4$ + 0.1 M $NaHCO_3$ and (b) 0.1 M $Na_2SO_4$ solutions at 25 °C (pH 8).

The role of bicarbonate in anodic dissolution can be explained by a dual effect: (i) by the lower solubility of the metal cations in the presence of $HCO_3^-/CO_3^{2-}$ and $SO_4^{2-}$ ions, and (ii) by the inhibition action as buffering ions to prevent the localized attack. The pitting and precipitation phenomena act at a microscopic scale (a few nanometres) and may not be detected on as large a scale as in the electrochemical measurements. The presence of $HCO_3^-/CO_3^{2-}$ ions in sulfate solutions has an inhibitive effect. Bicarbonate ions are also known for inhibiting pitting corrosion on stainless steel in chloride containing media [33].

Figure 18 presents the SS304 potentiodynamic traces in sulfate solutions with and without bicarbonate in the transpassive potential region before oxygen evolution. In the presence of $HCO_3^-/CO_3^{2-}$ ions, the anodic current increases from about 0.9 V and passes through a maximum at about 1.1 V. Depassivation of the SS304 surface without visible pitting is explained by Fe(III) to Fe(VI) oxidation, the reaction being activated by $HCO_3^-/CO_3^{2-}$ ions [25, 34–39]. The higher the bicarbonate concentration and temperature, the larger the anodic current peak, which indicates slow chemical steps involved in the oxidation process. Ferrate(VI) species generated at the oxide film enter into the solution but the anodic oxide film does not disappear and the SS304 surface repassivates. The fact that this anodic current peak does not exist in sulfate solutions at the same pH indicates that the $HCO_3^-/CO_3^{2-}$ ions play a key role in the stability of ferrate(VI) ion or complex removed from the electrode surface. The superficial ferrate in $HCO_3^-/CO_3^{2-}$ solution is more stable [25, 37–39], suggesting that the transpassive dissolution in metal–

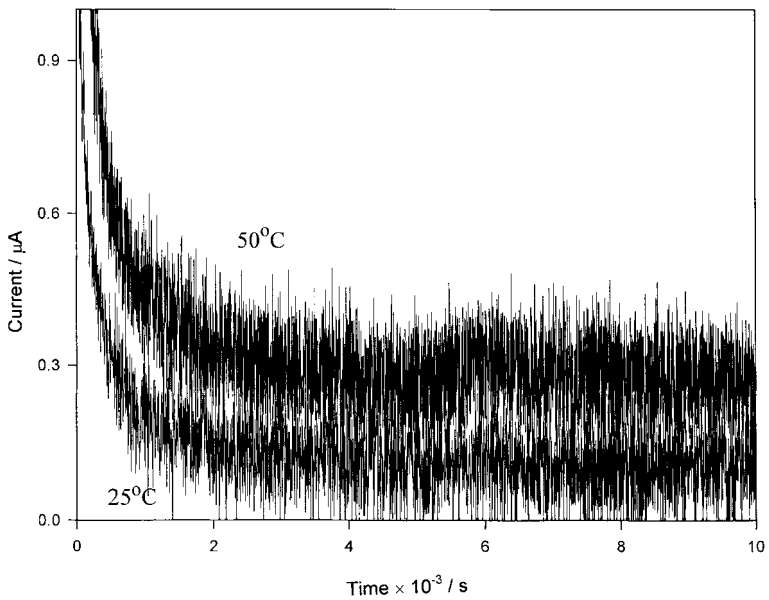


Fig. 15. As for Fig. 14 but in 0.1 M $Na_2SO_4$ + 0.1 M $NaHCO_3$ solution at 25 and 50 °C (pH 8).

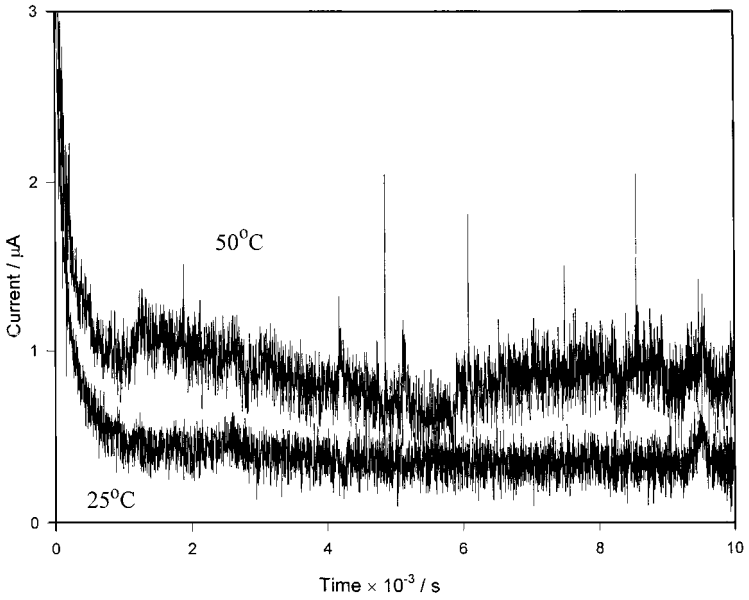


Fig. 16. As for Fig. 14 but in 0.5 M $Na_2SO_4$ + 0.1 M $NaHCO_3$ solution (pH 8).

electrolyte interface is governed by specific interactions between anode and electrolyte anions. It is proposed that the dissolution at high positive potentials proceeds through active patches in the passive film and involves direct transfer of ions from the metal lattice into the solution; the anion migrates through micropores or other defects in the anodic film and adsorbs at the metal surface [35]. There may also be a fixation of Fe(VI) species on the electrode surface.

## 4. Conclusion

SS304 electrode surfaces in 0.1–0.5 M $Na_2SO_4$ solutions at pH ~8 and at the potentials more positive than 0.4 V show evidence of microscopic pit nucle-

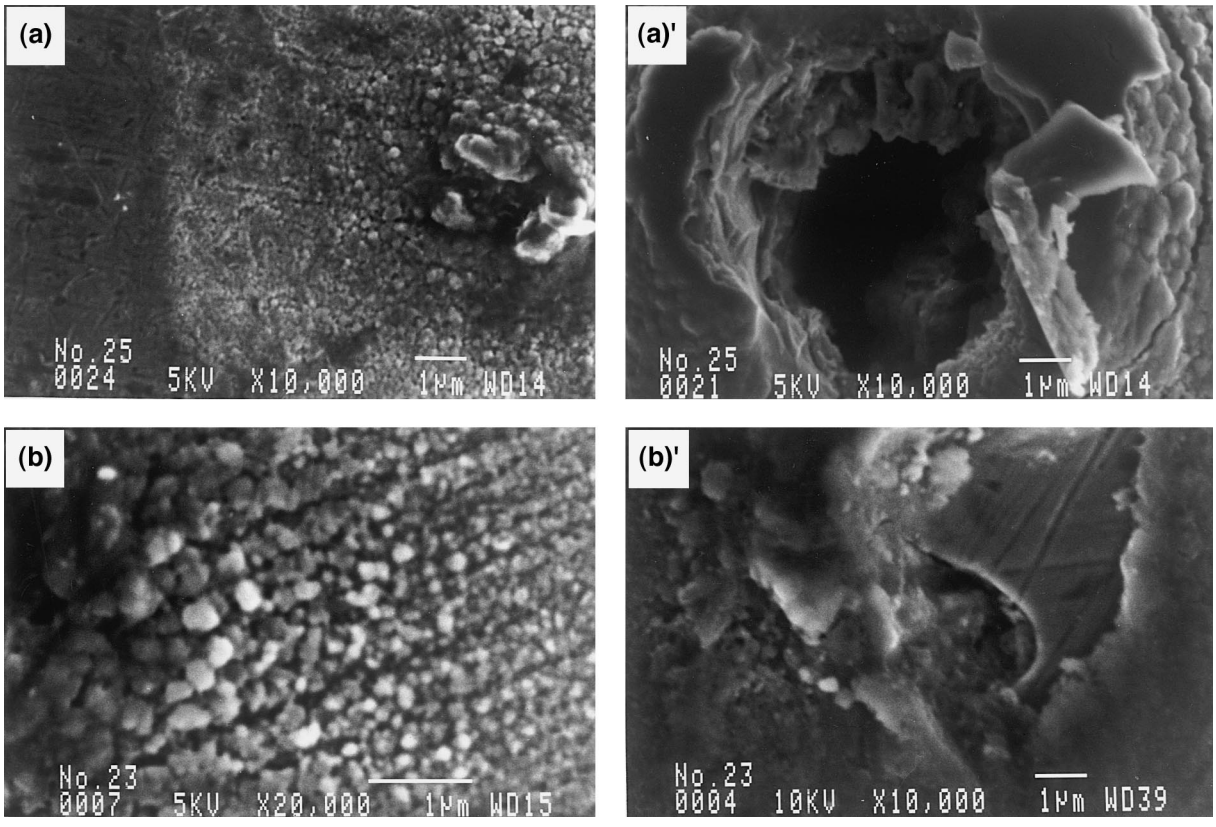


Fig. 17. SEM pictures for SS304 electrode surfaces after polarization at 0.8 V for 10 ks: (a) in 0.1 M $Na_2SO_4$ + 0.1 M $NaHCO_3$ solution at 25 °C; (a′) precipitate film and pit image finer resolution; (b) in 0.5 M $Na_2SO_4$ + 0.1 M $NaHCO_3$ solution at 25 °C; (b′) precipitate film and pit image finer resolution.

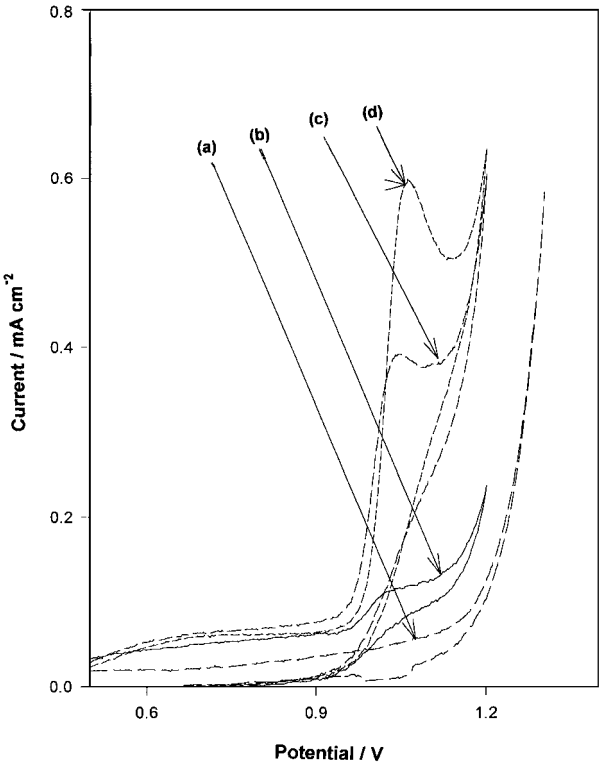


Fig. 18. Polarization curves of transpassive potential region for the SS304 electrode in 0.5 M $Na_2SO_4$, and 0.5 M $Na_2SO_4$ + $x$ M $NaHCO_3$ solutions ($x$ = (a) 0, (b) 0.01, (c) 0.05 (d) 0.1), at scan rate $E/dt$ = 5 mV s$^{-1}$, pH 8, 25 °C. Starting potential: −0.8 V.

ation. At 0.4 V, chromium oxy/hydroxide passive films dissolve from the SS304 surface. The SS304 surface structure with microscopic inclusions could be a cause of active site electrochemical and chemical dissolution. Pit nucleation does not lead to pit growth but pit nuclei die through repassivation immediately after birth. Passivation appears to be associated with the precipitation of a metal salt at the bottom of the pit and spreading to the top of the pit. The deposit on the interior of the pit was rich in manganese and the sulfur concentration increased on the surrounding surface adjacent to the pit.

Adding bicarbonate to the sulfate solutions protects the SS304 surface through precipitation of a thick metal salt and results in a low anodic passive current. The pH buffering capacity of the bicarbonate may have an effect on the formation of the surface oxy/hydroxy film, although the passivation is associated with mixed salt precipitation.

The increase of the anodic current in the transpassive potentials above about 0.9 V and the anodic current maximum observed at about 1.1 V are characteristic features for stainless steel, mild steel and iron in bicarbonate solution. The reaction is ascribed to the dissolution by the formation of ferrate(VI) ions and their stabilization by $HCO_3^-/CO_3^{2-}$ ions.

## Acknowledgements

This research was funded by Hydro-Québec (IREQ) and the Natural Sciences and Engineering Research Council of Canada.

## References

[1] S. Matsuda and H. H. Uhlig, *J. Electrochem. Soc.* **111** (1964) 156.
[2] H. Schwarz, *Werkst. Korros.* **16** (1965) 93.
[3] J. Honzak and D. Kuchynka, *ibid.* **21** (1970) 342.
[4] D. B. Gibbs and M. Cohen, *J. Electrochem. Soc.* **119** (1972) 416.
[5] S. Smialowska and G. Mrowczynski, *Br. Corros. J.* **10** (1975) 187.
[6] B. MacDougall, J. A. Bardwell and M. J. Graham, *in* 'Surface, Inhibition and Passivation' (edited by E. McCafferty and R. J. Brodd), The Electrochemical Society, Princeton, NJ (1986), p. 254.
[7] V. Kucera and E. Mattsson, *in* 'Corrosion Mechanism' (edited by F. Mansfeld), Marcel Dekker, New York (1987), p. 211.
[8] B. MacDougall and J. A. Bardwell, *J. Electrochem. Soc.* **135** (1988) 2437.
[9] H. S. Isaacs, *in* 'Advances in Localized Corrosion' (edited by H. S. Isaacs, U. Bertocci, J. Kruger and S. Smialowska), NASA, Houston, TX (1988), p. 221.
[10] A. A. Olowe and J. W. R. Génin, *Proc. Int. Sym. Sci. Engng*, CEBELCOR R T. **297** (1989) 363; *Corros. Sci.* **32** (1991) 965, 1021.
[11] T. E. Graedel and R. P. Frankenthal, *J. Electrochem. Soc.* **137** (1990) 2385.
[12] A. A. Olowe, B. Pauron and J. W. R. Génin, *Corros. Sci.* **32** (1991) 985.
[13] A. A. Olowe, P. Refait and J. W. R. Génin, *ibid.* **32** (1991) 1003.
[14] R. H. Jones, C. F. Windisch, B. W. Arey and D. R. Baer, *Corrosion* **47** (1991) 542.
[15] J. Gui and T. M. Devine, *Corros. Sci.* **36** (1994) 442.
[16] B. MacDougall, *in* 'Corrosion Mechanisms in Theory and Practice' (edited by P. Marcus and J. Oudar), Marcel Dekker, New York (1995), p. 143.
[17] G. Vatankhah, M. Drogowska, L. Brossard and H. Ménard, *J. Appl. Electrochem.*, in press.
[18] T. Beck, *J. Electrochem. Soc* **129** (1982) 2412.
[19] L. J. Simpson and C. A. Melendres, *J. Electrochem. Soc* **138** (1991) 1376
[20] R. Alkire, D. Ernsberger and T. R. Beck, *ibid.* **125** (1978) 1382.
[21] P. Russell, J. Newman, *ibid.* **133** (1986) 59.
[22] P. C. Pistorius and G. T. Burstein, *Corros. Sci.* **33** (1992) 1885; *idem*, *ibid.* **36** (1994) 525.
[23] J. Gui and T. M. Devine, *J. Electrochem. Soc.* **138** (1991) 1376; *idem*, *Corros. Sci.* **32** (1991) 1105.
[24] L. J. Oblonsky and T. M. Devine, *Corros. Sci.* **37** (1995) 17.
[25] M. Drogowska, L. Brossard and H. Ménard, *J. Appl. Electrochem.* **26** (1996) 217 and references therein.
[26] B. Elsener, D. DeFilippo and A. Rossi, *in* 'Surface Modification of Passive Films' (edited by P. Marcus, B. Baroux and M. Keddam). The Institute of Materials, London (1994), p. 6, EFC Publication No. 12.
[27] S. Tokansky, 'Multibeam Interference Microscopy of Metals', Academic Press, New York (1970).
[28] K. Massau, 'The Physics and Chemistry of Colors', Wiley Interscience, New York (1983).
[29] G. T. Burstein, P. C. Pistorius and S. P. Mattin, *Corros. Sci.* **35** (1993) 57.
[30] H. Böhni, T. Suter and A. Schreyer, *Electrochim. Acta* **40** (1995) 1361.
[31] T. Suter, T. Peter and H. Böhni, *Mater. Sci. Forum*, **192–194** (1995) 25.
[32] R. Ke and R. Alkire, *J. Electrochem. Soc.* **142** (1995) 4056.
[33] M. Drogowska, L. Brossard and H. Ménard, *J. Appl. Electrochem.* **27** (1997) 169.
[34] F. Beck, R. Kaus and M. Oberst, *Electrochim. Acta* **30** (1985) 173
[35] D. Landolt, *in* 'Passivity of Metals and Semiconductors' (edited by M. Froment), Elsevier Science, Amsterdam (1986), p. 484.
[36] J. P. Hoare, *ibid.*, p. 505.
[37] C. M. Rangel and R. A. Leitão, *Electrochim. Acta* **34** (1989) 255.
[38] C. M. Rangel, I. T. Fonseca and R. A. Leitão, *Electrochim. Acta* **31** (1986) 1659.
[39] K. Bouzek and I. Roušar, *J. Appl. Electrochem.* **23** (1993) 1317.